© APR 2026 | IRE Journals | Volume 9 Issue 10 | ISSN: 2456-8880
DOI: https://doi.org/10.64388/IREV9I10-1716456

Fourier-Transform Analysis of Electromagnetohydrodynamic Flow Over an Exponentially Stretching Sheet

OJO, ADETOYE SOLOMON[1], NWABUZOR, PETER ONYELUKACHUKWU[2]
[1]*Department of Physics, University of Port Harcourt, Choba, Nigeria*
ORCID ID: 0009-0005-3139-0704
[2]*Department of Physics with Electronics, University of Port Harcourt, Choba, Nigeria.*
ORCID ID: 0009-0001-2144-7245

Abstract- ***This study presents an exact analytical investigation of electromagnetohydrodynamic (EMHD) boundary-layer flow over an exponentially stretching surface, incorporating coupled heat and mass transfer with thermal radiation and magnetic field effects. The governing momentum, energy and concentration equations are transformed into normal coordinates and solved using a Fourier transform framework. Radiative heat flux is modeled via the Rosseland approximation, leading to a modified effective thermal diffusivity. Closed-form exponential expressions are obtained for the temperature and concentration distributions, while the velocity field is recovered through inverse Fourier transformation, accounting for thermal and solutal buoyancy coupling. The results indicate that temperature and concentration profiles exhibit exponential decay away from the surface, governed by radiation-modified Prandtl and Schmidt numbers. The applied magnetic field suppresses fluid motion, whereas thermal and solutal Grashof numbers enhance the velocity due to buoyancy effects. Increasing thermal radiation thickens the thermal boundary layer, reducing the Nusselt number and consequently the surface heat transfer rate, while higher Prandtl and Schmidt numbers significantly improve thermal and mass transport characteristics. Entropy generation analysis is performed to quantify thermodynamic irreversibility, revealing the combined influence of viscous dissipation and magnetic effects. The Bejan number distribution shows that heat transfer irreversibility dominates in the near-wall region. Furthermore, a multi-objective optimization framework is developed to simultaneously maximize heat transfer and minimize entropy production. The analysis demonstrates that optimal system performance is achieved at moderate Prandtl number, low radiation parameter and controlled magnetic field intensity. The present analytical solutions provide both physical insight and computational efficiency, offering a reliable framework for the design and optimization of advanced EMHD-based thermal-fluid systems.***

Indexed Terms- ***Electromagnetohydrodynamic Flow; Fourier Transform; Thermal Radiation (Rosseland Approximation); Exponentially Stretching Surface; Entropy Generation.***

I. INTRODUCTION

Electromagnetohydrodynamic (EMHD) flow has gained considerable attention due to its relevance in the study of electrically conducting fluids subjected to combined magnetic and electric fields. Such flows arise in numerous engineering and technological applications where electromagnetic forces interact with viscous fluid motion, thereby influencing momentum, heat, and mass transport processes. Previous studies have demonstrated that electromagnetic effects significantly alter velocity, temperature, and concentration distributions in conducting fluids (Ali et al., 2022; Adetoye et al., 2026; Sharma and Sood, 2022; Khan and Malik, 2023). As a result, the mathematical modeling of EMHD transport phenomena remains an active area of research in fluid mechanics and applied mathematics.

Boundary-layer flow over stretching surfaces constitutes a classical problem with wide applications in industrial processes such as polymer extrusion, wire drawing, continuous casting, and coating flows. The stretching motion induces strong velocity gradients, which significantly affect thermal and solutal transport within the boundary layer (Makinde and Eegunjobi, 2021; Gupta and Sharma, 2022). In particular, exponentially stretching surfaces introduce nonlinear spatial variations that complicate the governing equations and demand more advanced analytical or numerical solution techniques (Sharma and Sood, 2022; Singh and Patel, 2023).

Thermal radiation plays a crucial role in high-temperature heat transfer systems, including nuclear reactors, combustion chambers, and thermal insulation devices. In such situations, the classical energy equation must be modified to incorporate radiative heat flux, commonly modeled using the Rosseland diffusion approximation (Gupta and Sharma, 2022; Zhang and Li, 2024). The inclusion of radiation effects alters the effective thermal conductivity and typically increases the thermal boundary-layer thickness, thereby influencing the rate of heat transfer from the surface (Albqmi and Sivanandam, 2024; Das et al., 2023).

In recent years, entropy generation analysis has emerged as an important tool for evaluating thermodynamic irreversibility in heat and mass transfer processes. It provides a quantitative measure of energy degradation within a system and helps identify dominant sources of irreversibility, including heat transfer, viscous dissipation, Joule heating, and mass diffusion (Rahman and Alam, 2022; Reddy et al., 2024). In magnetohydrodynamic flows, these mechanisms collectively contribute to entropy generation and influence system performance (Asad, 2023; Ghaderi et al., 2024). Consequently, entropy analysis is widely used to assess and optimize the thermodynamic efficiency of fluid systems (Visweswara et al., 2025; Ahmed et al., 2024).

Closely related to entropy generation is the Bejan number, which represents the relative contribution of heat transfer irreversibility compared to fluid friction and magnetic dissipation. Higher values of the Bejan number indicate the dominance of heat transfer irreversibility, whereas lower values correspond to increased effects of viscous and magnetic dissipation (Rahman and Alam, 2022; Sakthi et al., 2024). Such thermodynamic indicators are essential for understanding and optimizing transport processes in EMHD systems.

From a mathematical standpoint, EMHD boundary-layer flows are governed by coupled nonlinear partial differential equations describing conservation of momentum, energy, and species concentration. Solving these equations presents significant challenges, and several approaches have been proposed, including similarity transformations, perturbation methods, homotopy analysis, and numerical discretization techniques (Singh and Patel, 2023; Khan and Malik, 2023). However, many of these methods rely heavily on numerical computation and often do not yield explicit analytical expressions that clearly reveal the influence of governing parameters.

Transform techniques offer a powerful alternative for obtaining analytical solutions to such problems. In particular, the Fourier transform method has been effectively used to convert differential equations into algebraic forms in spectral space, thereby simplifying the analytical solution process (Chen and Liu, 2026; Adeyemi and Ogunseye, 2025). Solutions derived through transform methods provide enhanced physical insight and allow direct examination of parameter effects in explicit functional form.

Despite the extensive literature on magnetohydrodynamic and EMHD flows, analytical studies based on transform techniques remain relatively scarce, especially for problems involving the combined effects of thermal radiation, coupled heat and mass transfer, entropy generation, and exponentially stretching surfaces (Ali et al., 2022; Albqmi and Sivanandam, 2024; Ahmed et al., 2024). Furthermore, many existing studies primarily focus on flow and thermal characteristics without incorporating thermodynamic optimization based on entropy generation and Bejan number analysis.

Motivated by these gaps, the present study develops a comprehensive analytical framework for EMHD boundary-layer flow over an exponentially stretching surface. The governing momentum, energy, and concentration equations are solved using the Fourier transform method to obtain closed-form solutions for velocity, temperature, and concentration fields. Thermal radiation is incorporated through the Rosseland approximation, while entropy generation and the Bejan number are evaluated to quantify thermodynamic irreversibility. The results provide detailed insights into the influence of key governing parameters, including magnetic field strength, radiation parameter, Prandtl number, and Schmidt number, on EMHD transport characteristics.

© APR 2026 | IRE Journals | Volume 9 Issue 10 | ISSN: 2456-8880
DOI: https://doi.org/10.64388/IREV9I10-1716456

II. MATHEMATICAL FORMULATION OF THE PROBLEM

Consider a steady, two-dimensional electromagnetohydrodynamic (EMHD) boundary-layer flow of an incompressible, electrically conducting fluid over an exponentially stretching surface. The surface is assumed to stretch with a velocity that varies exponentially along the axial direction. A uniform transverse magnetic field is applied, while the effects of thermal radiation and mass diffusion are incorporated into the analysis.

A Cartesian coordinate system (x, r) is adopted such that the x-axis is aligned along the stretching surface and the r-axis is taken normal to it. The corresponding velocity components in the x and $r$directions are denoted by $u$and v, respectively.

Under the boundary-layer approximations, the governing equations describing the conservation of mass, momentum, energy, and species concentration are expressed as follows:

Continuity equation

$$\frac{\partial u}{\partial x}+\frac{\partial v}{\partial r}=0 \tag{1}$$

Momentum equation

$$u\frac{\partial u}{\partial x}+v\frac{\partial u}{\partial r}=v\frac{\partial^2 u}{\partial r^2}-\frac{\sigma B_0^2}{\rho}v_r+g\beta_T\left(T-T_\infty\right)+g\beta_C\left(C-C_\infty\right) \tag{2}$$

Energy equation

$$u\frac{\partial T}{\partial x}+v\frac{\partial T}{\partial r}=K\frac{\partial^2 T}{\partial r^2}-\frac{1}{\rho C_p}\frac{\partial q_r}{\partial r} \tag{3}$$

Concentration equation

$$u\frac{\partial C}{\partial x}+v\frac{\partial C}{\partial r}=D\frac{\partial^2 C}{\partial r^2} \tag{4}$$

If the flow electromagnetohydrodynamic (EMHD) fluid flow over an exponentially stretching sheet is incompressible (steady state) equation (2) – (4) with the use of equation (1), transformed into

$$\frac{\mu}{\rho}\frac{\partial^2 v}{\partial r^2}-\frac{1}{\rho}\frac{\partial \rho}{\partial r}-\frac{\sigma B_0^2}{\rho}v_r+g\beta_T\left(T-T_\infty\right)+g\beta_C\left(C-C_\infty\right)=0 \tag{5}$$

$$\frac{D}{\rho C_p}\frac{\partial^2 C}{\partial r^2}-\frac{K_0 r^2 C}{\rho C_p}=0 \tag{6}$$

$$\frac{K}{\rho C_p}\frac{\partial^2 T}{\partial r^2}-\frac{1}{\rho C_p}\frac{\partial q_r}{\partial r}=0 \tag{7}$$

Where T is temperature, v is fluid velocity, ρ is fluid density, P is fluid pressure, μ is viscosity of fluid, q_r is radiation term, C_p is specific heat at constant pressure, K_0 is chemical reaction term, Kr is thermal conductivity of fluid, C is fluid concentration, D is chemical molecular diffusivity

III. ROSSELAND APPROXIMATION

Using the Rosseland diffusion approximation to consider the effect of a radiation an optically thick model in which the heat flux is

$$q_r=-\frac{4\sigma^*}{3k^*}\frac{\partial T^4}{\partial r} \tag{8}$$

where:

σ^* = Stefan–Boltzmann constant

k^* = mean absorption coefficient

Where K_B is the Stefan-Boltzmann constant and α is the absorption coefficient. It is assumed that the temperature difference within the flow is sufficiently small such that T^4 can be expressed as a linear function of temperature. This is accomplished by expanding T^4 in a Taylor series about T_∞ and neglect higher order terms, the expression results in to

$$T^4=4T_\infty^3 T-3T_\infty^4 \tag{8}$$

Then,

$$\frac{\partial T^4}{\partial r}=4T_\infty^3\frac{\partial T}{\partial r} \tag{9}$$

So the radiative heat flux becomes:

$$q_r=-\frac{16\sigma^* T_\infty^3}{3k^*}\frac{\partial T^4}{\partial r} \tag{10}$$

© APR 2026 | IRE Journals | Volume 9 Issue 10 | ISSN: 2456-8880
DOI: https://doi.org/10.64388/IREV9I10-1716456

Substitute into Energy Equation

$$\frac{K}{\rho C_p}\frac{\partial^2 T}{\partial r^2}-\frac{1}{\rho C_p}\frac{\partial q_r}{\partial r}=0 \tag{11}$$

$$-\frac{1}{\rho C_p}\frac{\partial q_r}{\partial r}=-\frac{16\sigma^* T_\infty^3}{3k^*}\frac{\partial^2 T}{\partial r^2} \tag{12}$$

So the energy equation becomes:

$$uT_x+vT_r=\left(\alpha+\frac{16\sigma^* T_\infty^3}{3k^*\rho C_p}\right)\frac{\partial^2 T}{\partial r^2} \tag{13}$$

IV. DIMENSIONAL ANALYSIS

To tackle the effect of the governing equations, therefore equation (5) – (7) are transmute into dimensionless form.

$$Sc^{-1}=\frac{D}{\rho C_p}, Gr=Gr_T\theta+Gr_c\phi, K_0=\frac{Kr^2\mu}{\rho C_p}, \mathrm{Re}^{-1}=\frac{\mu}{V_0 p}, \mathrm{Pr}^{-1}=\frac{K}{\rho C_p}$$

$$\rho=\frac{1}{\rho}\frac{\partial\rho}{\partial y}, \theta=\frac{T-T_\alpha}{T_b-T_\alpha}, R=\frac{16\varepsilon T_\alpha^3}{3\alpha(\rho C_p)}, \phi=\frac{C-C_\alpha}{C_b-C_\alpha}, S_0=\frac{k\left(T_w-T_\infty\right)^2}{T_\infty^2 L^2}$$

Where Re implies Reynolds profile, Pr represents Prandtl profile, Sc is Schmidt profile, $G_{r_T}\theta$ is thermal Grashofs number, $G_{r_c}\phi$ is modified Grashofs number, $\Re$ is dimensionless radiation term, θ is dimensionless temperature, C is dimensionless concentration.

Having employed the dimensionless parameters into equation (5), (6) and (13) transformed in to the form

$$\frac{\partial^2 v}{\partial r^2}-Mv+Gr\theta+Gr\phi=0 \tag{14}$$

$$\frac{1}{\mathrm{Pr}}\left(1+\frac{3}{4}R\right)\frac{\partial^2\theta}{\partial r^2}-k\theta=0 \tag{15}$$

$$\frac{1}{Sc}\frac{\partial^2\phi}{\partial r^2}-K_0\phi=0 \tag{16}$$

V. METHOD OF SOLUTION

Using the Fourier Transform Method as a solution technique to solve equation (14) – (16), then equation (10) can be

$$Sc^{-1}\frac{\partial^2\phi}{\partial r^2}-K_0\phi=0 \tag{17}$$

Boundary Conditions (Flat Exponentially Stretching Surface)

At the surface r = 0: $\phi(0)=1$

Far from the surface $r\to\infty$: $\phi(r)\to 0$ (18)

These conditions mean:

- Concentration is maximum at the surface
- It decays to ambient value far away

Rewrite the equation (17) multiply through by Sc:

$$\frac{\partial^2\phi}{\partial r^2}-ScK_0\phi=0 \tag{19}$$

Let: $\lambda^2=ScK_0$ (20)

Then the equation becomes:

$$\frac{\partial^2\phi}{\partial r^2}-\lambda^2\phi=0 \tag{21}$$

The Fourier Transform can be defined as

$$\hat{\phi}(k)=\int_{-\infty}^{\infty}\phi(r)e^{-ikr}dr \tag{22}$$

Using the Fourier transform property:

$$F\left(\frac{\partial^2\phi}{\partial r^2}\right)=-k^2\hat{\phi}(k) \tag{23}$$

Taking Fourier transform of the differential equation:

$$-k^2\hat{\phi}(k)-\lambda^2\hat{\phi}(k)=0$$

$$\hat{\phi}(k)\left(k^2+\lambda^2\right)=0 \tag{24}$$

Thus,

$$\hat{\phi}(k)=\frac{C}{k^2+\lambda^2} \tag{25}$$

Where C is a constant.

Inverse Fourier transform of equation (25) becomes

$$\phi(r)=\frac{1}{2\pi}\int_{-\infty}^{\infty}\frac{C}{k^2+\lambda^2}e^{ikr}dk \tag{26}$$

$$\int_{-\infty}^{\infty}\frac{e^{ikr}}{k^2+\lambda^2}dk=\frac{\pi}{\lambda}e^{-\lambda|r|} \tag{27}$$

Therefore,

$$\phi(r) = \frac{\pi}{\lambda} e^{-\lambda/r/} \tag{28}$$

Apply Boundary Conditions

Since $r \geq 0$ (physical region):

/r/ = r (29)

So:

$$\phi(r) = \frac{C}{2\lambda} e^{-\lambda r} \tag{30}$$

Apply surface condition $\phi(0) = 1$:

$$1 = \frac{C}{2\lambda}$$

$$C = 2\lambda \tag{31}$$

Final Solution implies

$$\phi(r) = e^{-\lambda r} \tag{32}$$

Where $\lambda = \sqrt{ScK_0}$

Equation (15) can be rewritten as

$$\Pr^{-1}\left(1 + \frac{3}{4}R\right)\frac{\partial^2\theta}{\partial r^2} - \beta\theta = 0 \tag{33}$$

Let $A = \frac{1}{\Pr}\left(1 + \frac{3}{4}R\right)$

Then the equation (33) becomes

$$\frac{\partial^2\theta}{\partial r^2} - \frac{\beta}{A}\theta = 0 \tag{34}$$

Let

$$\beta^2 = \frac{\beta}{A} \tag{35}$$

Thus

$$\frac{\partial^2\theta}{\partial r^2} - k^2\theta = 0 \tag{36}$$

Apply Fourier Transform

$\Theta(\omega) = \mathcal{F}[\theta(r)]$ (37)

Property of Fourier transform:

$\mathcal{F}\left[\frac{d^2\theta}{dr^2}\right] = -(\omega^2)\Theta(\omega)$ (38)

Substitute equation (37) 1nd (38) into the equation (36)

$A(-\omega^2)\Theta(\omega) - \lambda\Theta(\omega) = 0$ (39)

Take the factor of equation (39):

$\Theta(\omega)(-A\omega^2 - \lambda) = 0$ (40)

Thus

$\Theta(\omega) = \frac{C}{A\omega^2 + \lambda}$ (41)

Take Inverse Fourier Transform of equation (41)

Now compute

$\theta(r) = \mathcal{F}^{-1}\left[\frac{C}{A\omega^2 + \lambda}\right]$ (42)

Using the standard inverse transform identity:

$\mathcal{F}^{-1}\left[\frac{1}{\omega^2 + a^2}\right] = \frac{1}{2a}e^{-a|r|}$ (43)

where

$a = \sqrt{\frac{\lambda}{A}}$ (44)

Thus

$\theta(r) = C_1 e^{-\beta r} + C_2 e^{\beta r}$ (45)

Where

$\beta = \sqrt{\frac{\lambda Pr}{1 + \frac{3}{4}R}}$ (46)

Final Analytical Solution of equation (45) gives

$\theta(r) = C_1 e^{-r\sqrt{\frac{\lambda Pr}{1+\frac{3}{4}R}}} + C_2 e^{r\sqrt{\frac{\lambda Pr}{1+\frac{3}{4}R}}}$ (47)

Apply Typical Boundary Conditions (Thermal Boundary Layer)

For EMHD cylindrical surface problems usually:

$$\theta(0) = 1, \theta(\infty) = 0$$

From $\theta(\infty) = 0$, the growing exponential vanishes: $C_2 = 0$

Final Temperature Profile

$$\theta(r) = \exp\left(-\sqrt{\frac{\Pr\lambda}{1 + \frac{4}{3}R}}\, r\right) \tag{48}$$

Equation (14) can be rewritten as

$$\frac{\partial^2 v}{\partial r^2} - Mv + Gr_\theta e^{-\beta r} + Gr_\phi e^{-\lambda r} = 0 \tag{49}$$

Fourier transform for velocity equation can be defined as

$$\hat{v}(k)=\int_{-\infty}^{\infty} v(r)e^{-ikr}dr \tag{50}$$

Using transform properties:

$$F\left(\frac{\partial^2 v}{\partial r^2}\right)=-k^2\hat{v}(k) \tag{51}$$

Taking Fourier transform of equation (49) it gives

$$-k^2\hat{v}(k)-M\hat{v}(k)+\frac{Gr_\theta}{k^2+\beta^2}+\frac{Gr_\phi}{k^2+\lambda^2}=0 \tag{52}$$

$$\hat{v}(k)=\frac{\dfrac{Gr_\theta}{k^2+\beta^2}+\dfrac{Gr_\phi}{k^2+\lambda^2}}{k^2+M} \tag{53}$$

$$\hat{v}(k)=\frac{Gr_\theta}{\left(k^2+M\right)\left(k^2+\beta^2\right)}+\frac{Gr_\phi}{\left(k^2+M\right)\left(k^2+\lambda^2\right)} \tag{54}$$

Applying Inverse Fourier transform in equation (54) with the following identities

$$F^{-1}\left(\frac{1}{\left(k^2+a^2\right)\left(k^2+b^2\right)}\right)=\frac{1}{a^2-b^2}\left[\frac{e^{-br}}{2b}-\frac{e^{-ar}}{2a}\right] \tag{55}$$

Using equation (54) in equation (55) the result yields

$$v_1(r)=\frac{Gr_\theta}{M-\beta^2}\left[\frac{e^{-\beta r}}{2\beta}-\frac{e^{-\sqrt{M}r}}{2\sqrt{M}}\right] \tag{56}$$

$$v_2(r)=\frac{Gr_\phi}{M-\lambda^2}\left[\frac{e^{-\lambda r}}{2\lambda}-\frac{e^{-\sqrt{M}r}}{2\sqrt{M}}\right] \tag{57}$$

Combine equation (56) and (57) together it gives

$$v(r)=\frac{Gr_\theta}{M-\beta^2}\left[\frac{e^{-\beta r}}{2\beta}-\frac{e^{-\sqrt{M}r}}{2\sqrt{M}}\right]+\frac{Gr_\phi}{M-\lambda^2}\left[\frac{e^{-\lambda r}}{2\lambda}-\frac{e^{-\sqrt{M}r}}{2\sqrt{M}}\right] \tag{58}$$

Apply boundary conditions

For exponentially stretching surface:

At r = 0, v (0) = V_w (59)

Far field condition is satisfied automatically.

VI. OPTIMIZATION AND APPLICATION OF ELECTROMAGNETOHYDRODYNAMIC FLUID FLOW

Optimization of electromagnetohydrodynamic (EMHD) fluid flow plays a critical role in enhancing heat and mass transfer in electrically conducting fluids through the effective control of key governing parameters, including magnetic field intensity and thermal radiation effects. In the present study, the Fourier transform method is employed to obtain analytical solutions, enabling clear identification of optimal conditions for improved transport performance. Optimized EMHD flow systems have wide-ranging applications in engineering and technology, including electromagnetic pumping, advanced cooling systems, metallurgical processing, and microfluidic devices, where precise control of fluid motion and thermal characteristics is essential. The analysis reveals that optimal system performance can be achieved under appropriate combinations of governing parameters, as outlined below:

6.1 Effective Thermal Diffusivity

The effective thermal diffusivity represents the modified capacity of the fluid to conduct and diffuse heat in the presence of additional physical effects, particularly thermal radiation. It accounts for the combined contribution of classical molecular heat conduction and radiative heat transfer within the fluid medium. This parameter plays a key role in governing the rate at which temperature variations propagate through the boundary layer and, consequently, strongly influences the overall heat transfer characteristics of the system. Mathematically, the effective thermal diffusivity is expressed as:

$$\alpha_{eff}=\alpha\left(1+\frac{4}{3}R\right) \tag{60}$$

Where the radiation parameter R is

$$R=\frac{4\sigma^* T_\infty^3}{kk^*} \tag{61}$$

6.2 Sherwood number

This parameter represents the rate of mass transfer from the stretching surface into the surrounding fluid. It is a dimensionless quantity that characterizes the relative dominance of convective mass transport over molecular diffusion within the boundary layer. A higher Sherwood number corresponds to enhanced mass transfer rates and a thinner concentration boundary layer in the vicinity of the surface.

© APR 2026 | IRE Journals | Volume 9 Issue 10 | ISSN: 2456-8880
DOI: https://doi.org/10.64388/IREV9I10-1716456

$$Sh = -\left.\frac{d\phi}{dr}\right|_{r=0} = \lambda = \sqrt{ScK_0} \tag{62}$$

6.3 Nusselt number

The Nusselt number (Nu) characterizes the rate of heat transfer from the stretching surface to the adjacent fluid within the boundary layer. It is a dimensionless parameter that represents the ratio of convective heat transfer to conductive heat transfer at the surface. In electromagnetohydrodynamic (EMHD) flow over an exponentially stretching sheet, the Nusselt number indicates the effectiveness of thermal energy transport from the surface into the electrically conducting fluid. A higher Nusselt number signifies enhanced heat transfer at the surface, leading to a thinner thermal boundary layer and more efficient heat removal from the stretching sheet.

$$Nu = \sqrt{\frac{\Pr\lambda}{1+\frac{4}{3}R}} \tag{63}$$

6.4 Skin friction coefficient

The skin friction coefficient is a dimensionless parameter that quantifies the shear stress exerted by the fluid on the stretching surface due to its motion. It represents the resistance offered by the fluid to the movement of the surface and is directly related to the velocity gradient at the wall. In electromagnetohydrodynamic (EMHD) flow, the skin friction coefficient provides insight into the influence of the magnetic field, boundary forces, and other governing parameters on the near-wall flow behavior. A higher value of the skin friction coefficient indicates increased frictional drag between the fluid and the stretching sheet.

$$C_f = \left.\frac{dv}{dr}\right|_{r=0} \tag{64}$$

Differentiating the velocity solution gives

$$C_f = \frac{Gr_\theta}{M-\beta^2}\left(-\frac{1}{2}+\frac{\beta}{2\sqrt{M}}\right)+\frac{Gr_\phi}{M-\lambda^2}\left(-\frac{1}{2}+\frac{\lambda}{2\sqrt{M}}\right) \tag{65}$$

VII. ENTROPY GENERATION ANALYSIS

Entropy generation represents the thermodynamic irreversibility occurring within the fluid system. It quantifies the rate of energy degradation resulting from heat transfer, viscous dissipation, magnetic effects, and mass diffusion. Through entropy generation analysis, it becomes possible to identify the dominant mechanisms responsible for energy loss and system inefficiency. This analysis is particularly important in electromagnetohydrodynamic (EMHD) flows, as it provides a basis for optimizing operating conditions that enhance heat and mass transfer while minimizing irreversibility, thereby improving overall thermal-fluid performance. The dimensional local entropy generation rate is expressed as follows:

$$S_{gen}''' = \frac{k}{T_\infty^2}\left(\frac{\partial T}{\partial r}\right)^2 + \frac{\mu}{T_\infty}\left(\frac{\partial v}{\partial r}\right)^2 + \frac{\sigma B_0^2}{T_\infty}v^2 + \frac{D}{T_\infty}\left(\frac{\partial C}{\partial r}\right)^2 \tag{66}$$

Applying dimensionless analysis on equation (66) it becomes entropy generation number

$$N_s = \left(\frac{\partial\theta}{\partial r}\right)^2 + Br\left(\frac{\partial v}{\partial r}\right)^2 + Mv^2 + \Gamma\left(\frac{\partial\phi}{\partial r}\right)^2 \tag{67}$$

VIII. EXACT SOLUTIONS

Exact solutions refer to closed-form analytical expressions for the velocity, temperature, and concentration fields that exactly satisfy the governing differential equations together with the associated boundary conditions. These solutions provide valuable physical insight into the influence of key flow parameters on the system behavior. In addition, they enable the precise evaluation of important engineering quantities such as the Nusselt number, Sherwood number, and skin friction coefficient.

Recall

$$\theta = e^{-\beta r} \tag{68}$$

$$\phi = e^{-\lambda r} \tag{69}$$

$$v(r) = \text{(sum of exponential terms)}$$

Solve the first derivative of equation (68) and (69)

$$\frac{\partial\theta}{\partial r} = -\beta e^{-\beta r} \tag{70}$$

$$\frac{\partial\phi}{\partial r} = -\lambda e^{-\lambda r} \tag{71}$$

Solve the second derivative of equation (70) and (71)

$$\left(\frac{\partial\theta}{\partial r}\right)^2 = \beta^2 e^{-2\beta r} \tag{72}$$

© APR 2026 | IRE Journals | Volume 9 Issue 10 | ISSN: 2456-8880
DOI: https://doi.org/10.64388/IREV9I10-1716456

$$\left(\frac{\partial \phi}{\partial r}\right)^2 = \lambda^2 e^{-2\lambda r} \tag{73}$$

Substitute equation (72) – (73) into (67) which gives the final entropy generation expression

$$N_s = \beta^2 e^{-2\beta r} + Br\left(\frac{\partial v}{\partial r}\right)^2 + Mv^2 + \Gamma\lambda^2 e^{-2\lambda r} \tag{74}$$

IX. BEJAN NUMBER

The Bejan number is a dimensionless parameter that quantifies the relative contribution of heat transfer irreversibility to the total entropy generation within a system. A Bejan number approaching unity indicates that heat transfer effects dominate the irreversibility mechanisms, whereas values close to zero signify that fluid friction and magnetic effects are the primary contributors. In electromagnetohydrodynamic (EMHD) flows, the Bejan number serves as an important diagnostic tool for evaluating and optimizing the thermodynamic efficiency of the system.

$$Be = \frac{Heat\ transfer\ irreversibility}{Total\ irreversibility} \tag{75}$$

X. RESULTS AND DISCUSSION

The analytical solutions obtained for the velocity, temperature, and concentration fields are analyzed to investigate the influence of key governing parameters on the electromagnetohydrodynamic (EMHD) boundary-layer flow. In particular, the effects of the magnetic parameter M, radiation parameter R, Prandtl number Pr, Schmidt number Sc, and buoyancy-related parameters are examined in detail. The results are presented graphically to illustrate the physical behavior of the flow and transport characteristics under varying parameter conditions.

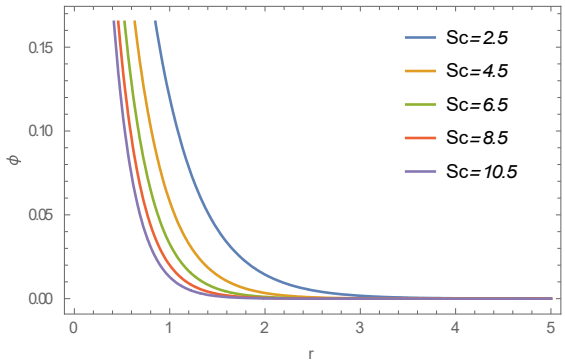

Figure 1. Concentration profile ϕ against boundary layer r for varying Schmidt number Sc.

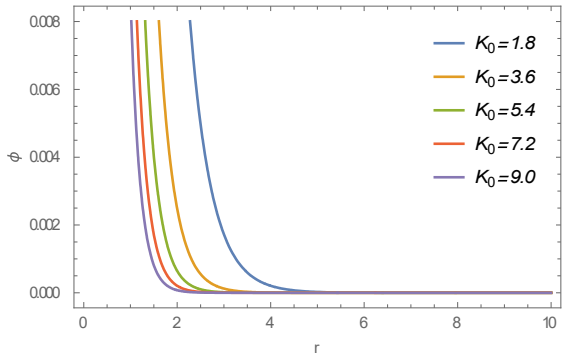

Figure 2. Concentration profile ϕ against boundary layer r for varying Chemical reaction term K_0.

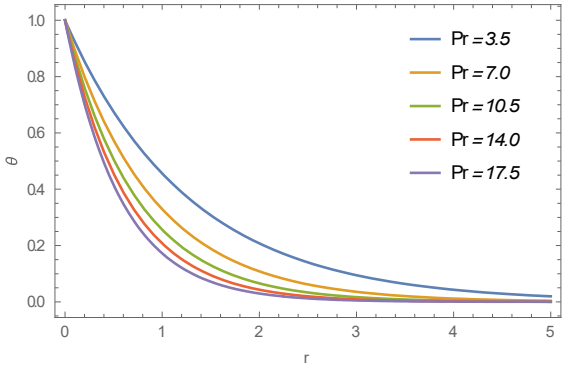

Figure 3. Temperature profile θ against boundary layer r for varying Prandtl number Pr.

© APR 2026 | IRE Journals | Volume 9 Issue 10 | ISSN: 2456-8880
DOI: https://doi.org/10.64388/IREV9I10-1716456

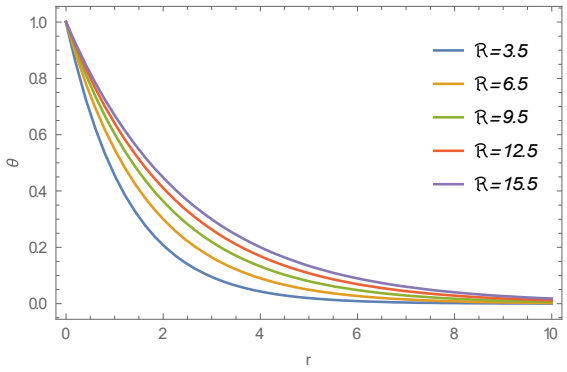

Figure 4. Temperature profile θ against boundary layer r for varying Radiation parameter R.

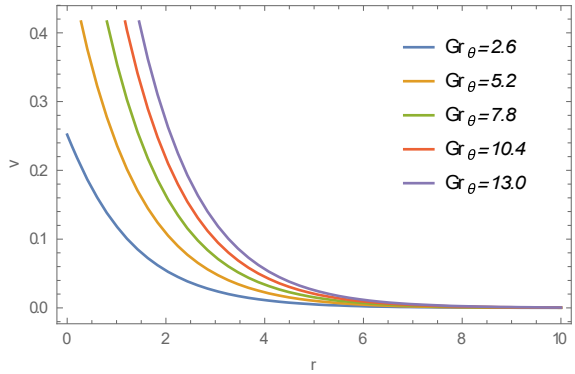

Figure 5. Velocity profile v against boundary layer r for varying Grashof number in term of temperature Gr_θ.

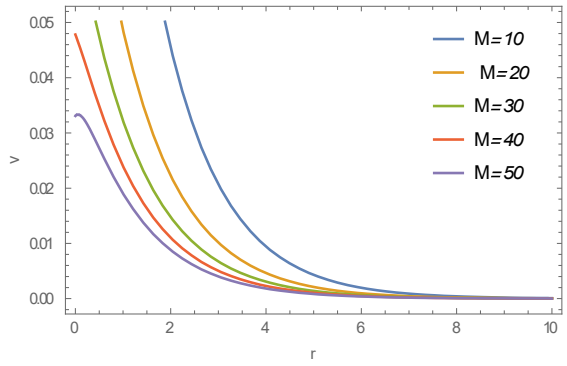

Figure 6. Velocity profile v against boundary layer r for varying Magnetic parameter (M).

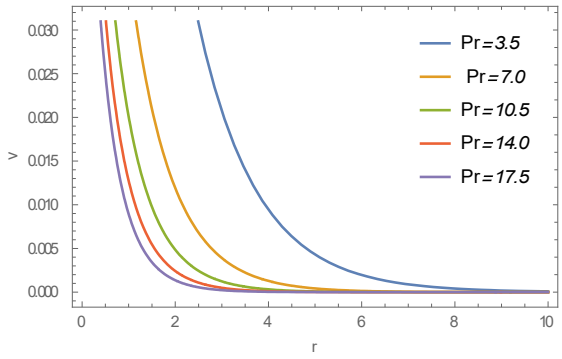

Figure 7. Velocity profile v against boundary layer r for varying Prandtl number Pr.

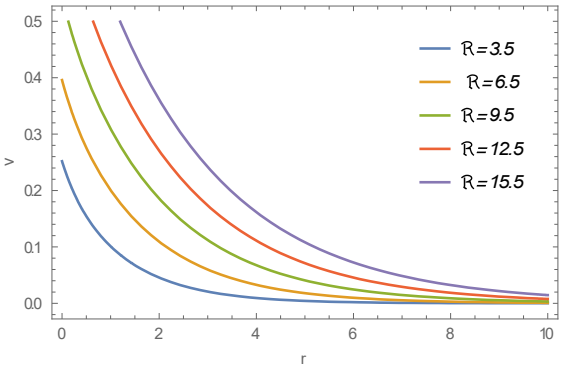

Figure 8. Velocity profile v against boundary layer r for varying Radiation parameter R.

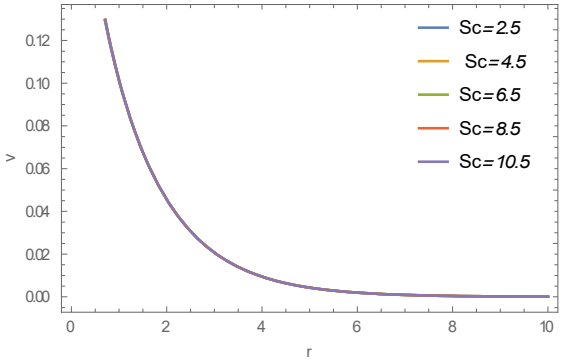

Figure 9. Velocity profile v against boundary layer r for varying Schmidt number Sc.

© APR 2026 | IRE Journals | Volume 9 Issue 10 | ISSN: 2456-8880
DOI: https://doi.org/10.64388/IREV9I10-1716456

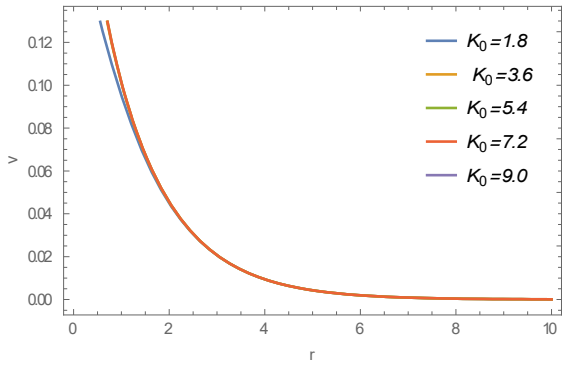

Figure 10. Velocity profile v against boundary layer r for varying Chemical reaction term K_0.

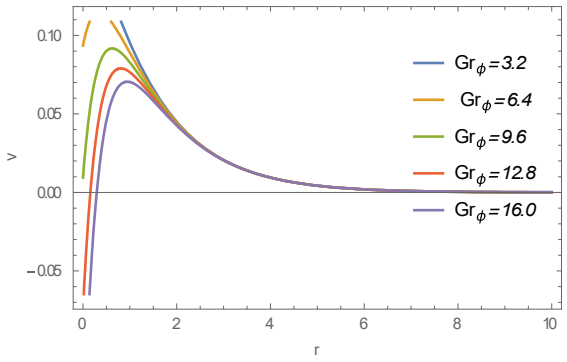

Figure 11. Velocity profile v against boundary layer r for varying Grashof number in term of concentration Gr_ϕ.

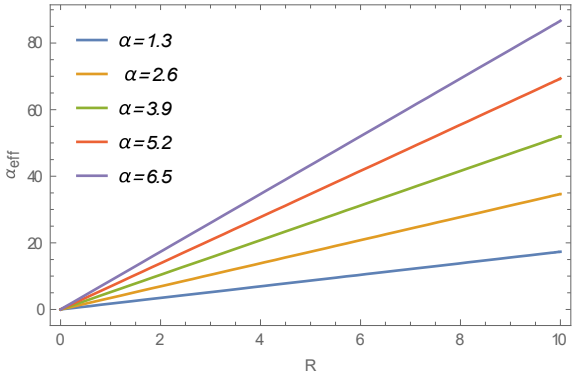

Figure 12. Effective Thermal Diffusivity profile α_{eff} against Radiation (R)

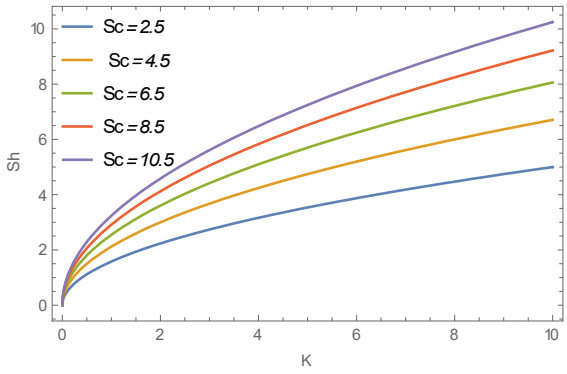

Figure 13. Sherwood profile (Sh) against Chemical reaction (K)

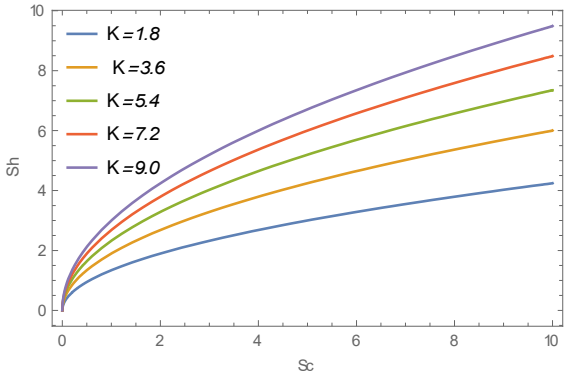

Figure 14. Sherwood profile (Sh) against Schmidt number (Sc)

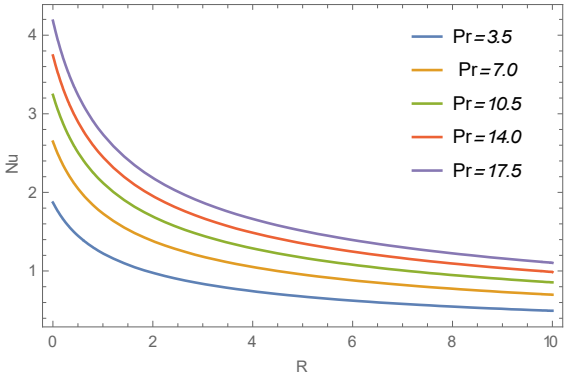

Figure 15. Nusselt number (Nu) against Radiation parameter (R)

© APR 2026 | IRE Journals | Volume 9 Issue 10 | ISSN: 2456-8880
DOI: https://doi.org/10.64388/IREV9I10-1716456

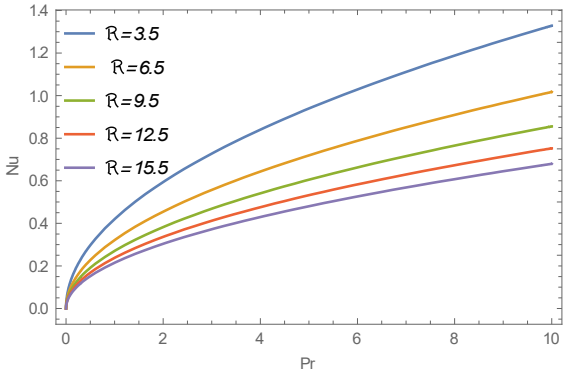

Figure 16. Nusselt number (Nu) against Prandtl parameter (Pr)

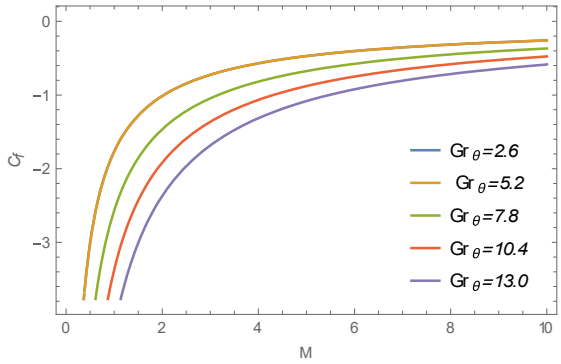

Figure 17. Skin friction (C_f) against Grashof number in term of temperature Gr_θ.

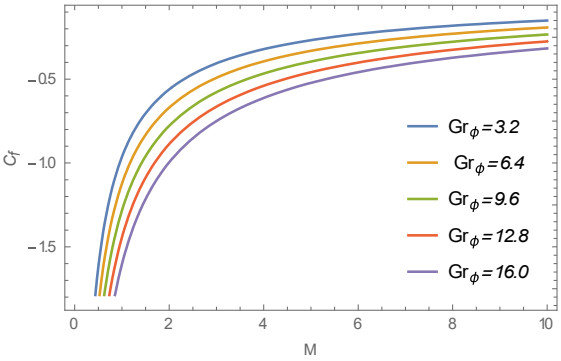

Figure 18. Skin friction (C_f) against Grashof number in term of concentration Gr_ϕ.

Figure 1 shows how the concentration profile ϕ changes with the boundary layer coordinate r for different Schmidt number Sc values. The concentration decreases as the distance from the stretching surface increases, meeting the far-field boundary conditions. A higher Sc significantly limits the concentration distribution within the boundary layer. This is because increased Schmidt numbers reduce mass diffusivity, which weakens species diffusion and leads to a thinner concentration boundary layer. On the other hand, lower Sc values allow for greater mass diffusion, resulting in a thicker concentration layer. This behavior aligns with classical mass transfer theory and is important in processes like polymer extrusion and coating technologies, where controlling species transport is crucial.

Figure 2 depicts the effect of the chemical reaction parameter K_0 on the concentration profile. The concentration decreases with increasing r. Higher K_0 value cause a noticeable drop in species concentration within the boundary layer because stronger chemical reactions speed up the consumption of diffusing species, thinning the concentration boundary layer. Such that the behavior is vital in catalytic reactions, chemical reactors, and surface treatment processes.

Figure 3 presents the temperature profile θ for different Prandtl number Pr values. The temperature decreases as the distance from the surface increases. A higher Prandtl number (Pr) reduces the thermal distribution in the boundary layer due to lower thermal diffusivity, which restricts heat propagation and results in a thinner thermal boundary layer. This phenomenon is significant for thermal management applications, such as polymer processing and electronic cooling systems.

Figure 4 shows the impact of the radiation parameter R on temperature distribution. As R increases, the temperature rises, indicating that thermal radiation improves energy transport in the fluid. This results in a thicker thermal boundary layer due to extra radiative heat transfer. This effect is especially relevant in high-temperature industrial processes such as glass manufacturing and thermal coating operations.

Figure 5 illustrates how the thermal Grashof number Gr_θ affects velocity distribution. The velocity increases with Gr_θ because enhanced buoyancy forces from temperature differences accelerate fluid motion and thicken the momentum boundary layer. This is important in natural convection systems and thermal engineering applications.

Figure 6 demonstrates the influence of the magnetic parameter M on velocity. Increasing M lowers the velocity due to the Lorentz force, which opposes fluid motion and slows down the flow. As a result, the momentum boundary layer becomes thinner. This behavior is commonly seen in electromagnetic flow control and MHD-based industrial systems.

Figure 7. highlights the effect of the Prandtl number on velocity. A slight decrease in velocity is noted with increasing Pr, caused by reduced thermal diffusion and weaker buoyancy effects in thermally coupled flows, which leads to a slight thinning of the momentum boundary layer.

Figure 8. shows how the radiation parameter R influences velocity. Increasing R boosts velocity due to added thermal energy in the fluid, which strengthens buoyancy forces and thickens the momentum boundary layer.

Figure 9 depicts the effect of the Schmidt number Sc on velocity. Higher Sc slightly reduces velocity because lower mass diffusivity weakens species-momentum interaction and thins the momentum boundary layer.

Figure 10 shows the effect of chemical reaction parameter K_0 on velocity. Increasing K_0 decreases velocity due to enhanced species consumption, which suppresses flow development and reduces boundary layer thickness.

Figure 11 demonstrates the effect of solutal Grashof number Gr_ϕ on velocity. Increasing Gr_ϕ enhances velocity due to stronger concentration-induced buoyancy forces, resulting in a thicker momentum boundary layer.

Figure 12 presents the variation of effective thermal diffusivity α_{eff} with radiation parameter R. It is observed that α_{eff} upsurges with R, indicating enhanced heat transport due to radiative effects, which thickens the thermal boundary layer.

Figure 13 shows the variation of Sherwood number $Sh$with chemical reaction parameter K. Increasing K reduces Sh, indicating suppressed mass transfer due to stronger species consumption at the surface.

Figure 14 illustrates the effect of Schmidt number Scon Sherwood number. Increasing Sc enhances Sh, indicating improved mass transfer due to steeper concentration gradients and reduced diffusivity.

Figure 15 presents the Nusselt number Nuas a function of radiation parameter R. Increasing Renhances Nu, indicating improved heat transfer due to stronger thermal radiation effects that increase temperature gradients near the surface.

Figure 16 shows the effect of Prandtl number on Nusselt number. Increasing Princreases Nu, as lower thermal diffusivity enhances temperature gradients and improves heat transfer rate.

Figure 17 illustrates the skin friction coefficient C_f versus thermal Grashof number Gr_θ. Increasing Gr_θ increases C_f, indicating higher shear stress due to stronger buoyancy-driven flow.

Figure 18 shows the effect of solutal Grashof number Gr_ϕ on skin friction coefficient. Increasing Gr_ϕ enhances C_f, as concentration-driven buoyancy increases flow velocity and surface shear.

CONCLUSION

This study looked at the effect of key physical parameters on electromagnetohydrodynamic (EMHD) boundary-layer flow over an exponentially stretching sheet using a Fourier-transform analytical method. The results provide valuable insights into the interaction of momentum, heat, and mass transfer influenced by magnetic fields, radiation, buoyancy forces, and chemical reactions.

The main conclusions are summarized as follows:

- The Schmidt number Sc and chemical reaction parameter K_0 significantly reduce concentration distribution, leading to a thinner concentration boundary layer due to suppressed mass diffusion and enhanced species consumption.
- The Prandtl number $Pr$and radiation parameter R strongly influence thermal behavior, where higher

Pr reduces thermal diffusion while higher R enhances heat transport, thereby controlling thermal boundary layer thickness.

- Thermal and solutal Grashof numbers (Gr_θ, Gr_ϕ) and radiation parameter Renhance velocity and momentum boundary layer thickness, whereas magnetic parameter M, higher Sc, and chemical reactions suppress flow development due to Lorentz forces and reduced diffusion effects.
- Nusselt number Nu and Sherwood number Shincrease with radiation, Prandtl, and Schmidt numbers, indicating improved heat and mass transfer under optimized conditions.
- Skin friction coefficient C_f increases with buoyancy effects, highlighting stronger surface shear stress in thermally and solutally driven flows, which is important for process optimization in EMHD systems.

Overall, the study shows that controlling the key parameters allows for effective improvement of heat transfer, mass transfer, and performance related to entropy in EMHD flow systems.

REFERENCES

[1] Adeyemi, O., & Ogunseye, H. (2025). Analytical solutions of electromagnetohydrodynamic boundary layer equations. *Applied Mathematics Letters, 150*, 109123. https://doi.org/10.1016/j.aml.2025.109123

[2] Ahmed, H., Biswas, S., & Tina, F. (2024). Mixed convection and entropy generation in nanofluid flow systems. *International Journal of Thermal Sciences, 197*, 108721. https://doi.org/10.1016/j.ijthermalsci.2024.108721

[3] Albqmi, N. M., & Sivanandam, S. (2024). Entropy generation and thermal radiation impact on magneto-convective hybrid nanofluid flow. *Computation, 12*(3), Article 43. https://doi.org/10.3390/computation12030043

[4] Ali, A., Khan, H. S., Saleem, S., & Hussan, M. (2022). EMHD nanofluid flow with radiation and variable heat flux effects along a stretching sheet. *Nanomaterials, 12*(21), Article 3872. https://doi.org/10.3390/nano12213872

[5] Adetoye S. Ojo, Peter O. Nwabuzor, Chijioke A. Egbo., & Edikan S. Umoh. (2026). The Application of Homotopy Perturbation Method in Newtonian Fluids. *Fluid Mechanics,* Vol 11(1), pp 1-11. http://www.sciencepg.com/journal/fm.

[6] Asad, S. (2023). Nonlinear stretched flow of a radiative MHD Prandtl fluid with entropy generation. *Frontiers in Physics, 11*, Article 1178296. https://doi.org/10.3389/fphy.2023.1178296

[7] Chen, X., & Liu, P. (2026). Advanced analytical methods for nonlinear heat and mass transfer systems. *Mathematics and Computers in Simulation, 221*, 318–332. https://doi.org/10.1016/j.matcom.2024.02.015

[8] Das, R., Sakthi, I., & Reddy, B. (2023). Entropy generation in radiative MHD hybrid nanofluid flow. *Numerical Heat Transfer, Part B: Fundamentals, 84*(4), 351–368. https://doi.org/10.1080/10407790.2023.2215948

[9] Ghaderi, E., Bijarchi, M., & Hannani, S. (2024). Joule heating and entropy generation in magnetohydrodynamic flows. *Physics of Fluids, 36*(2), 023602. https://doi.org/10.1063/5.0187564

[10] Gupta, P., & Sharma, R. (2022). Radiative heat transfer effects in electrically conducting fluid flows. *Heat Transfer Engineering, 43*(14), 1298–1312. https://doi.org/10.1080/01457632.2021.195724

[11] Khan, M., & Malik, M. (2023). Analytical investigation of MHD boundary layer flows with heat and mass transfer. *Applied Mathematics and Computation, 438*, 127912. https://doi.org/10.1016/j.amc.2023.127912

[12] Makinde, O. D., & Eegunjobi, A. S. (2018). Entropy analysis in MHD flow with heat source and thermal radiation past a stretching sheet in a porous medium. *Defect and Diffusion Forum, 387*, 364–372. https://doi.org/10.4028/www.scientific.net/DDF.387.364

[13] Rahman, M., & Alam, M. (2022). Thermodynamic analysis of entropy generation in magnetized flows. *Entropy, 24*(8)

[14] Sakthi, I., Das, R., & Reddy, P. B. A. (2024). Entropy generation on MHD flow of second-grade hybrid nanofluid over a converging/diverging channel: An application in hyperthermia therapeutic aspects. *The European Physical Journal Special Topics, 233*(6), 1233–1249. https://doi.org/10.1140/epjs/s11734-024-01117-y

[15] Sharma, D., & Sood, S. (2022). Radiation and slip effects on nanofluid MHD flow past an exponentially stretched surface. *International Journal of Heat and Mass Transfer*. Advance online publication. https://arxiv.org/abs/2211.04028

[16] Singh, A., & Patel, N. (2023). Spectral methods for boundary layer transport equations. *Applied Mathematical Modelling, 112*, 123–145.

[17] Visweswara, S., Palani, B., Al Mukahal, F. H. H., Raju, S. S. K., Souayeh, B., & Varma, S. V. (2025). Thermal entropy generation in magnetized radiative flow through porous media over a stretching cylinder: An RSM-based study. *Mathematics, 13*(19), Article 3189. https://doi.org/10.3390/math13193189

[18] Zhang, Y., & Li, J. (2024). Mathematical modeling of radiative magnetohydrodynamic transport processes. *Physics of Fluids, 36*(4), 043.